

Chapter 2

Fundamental Radial Velocity

The radial velocity method, has been a consistent power-horse for the measurement of the orbital motion of binary stars and stars hosting exoplanets. In this chapter some of the key properties of Keplerian orbits and the RV signal will be presented along with an introduction to the notion of RV precision.

2.1 Keplerian Orbits

When two bodies are in orbit (two stars or a star and a planet) they orbit about their common centre of mass. Their 3-dimensional motion can be derived with a combination of Newton's universal law of gravitation, and Kepler's laws. The full derivation is quite long and can be commonly found in several celestial mechanics texts (e.g. Moulton, 1914; M. Perryman, 2011; Fitzpatrick, 2012). The notes given here mainly follow (Bozza et al., 2016).

Figure 2.1 shows the basic elements of the Keplerian orbit. There are several parameters required to situate the orbit in space. There is a *reference plane*, tangential to the celestial sphere, that cuts the orbital plane with a *line of nodes*. The *ascending node* is the point on the plane at which the body crosses the reference plane moving away from the observer, and is defined relative to the vernal reference point, Υ , with the *longitude of the ascending node*, Ω , setting the orientation.

To fully parametrize a Keplerian orbit requires seven parameters. These are: a the semi-major axis of the elliptical orbit, e the orbital eccentricity, P orbital period, T_0 the *time of periastron passage*, i orbital inclination relative to the line of sight, ω the *argument of periastron*, and Ω . From RV measurements alone all of these parameters except for i and Ω can be determined. Ω is irrelevant for determining the orbital mass, but inclination i is very important as it effects the projection of the velocity towards the observer.

With a two body system with masses M_1 and M_2 , under the force of gravity, their orbits are elliptical orbit about their barycentre mass, as seen in Figure 2.2. In polar coordinates the ellipse of an orbit about the centre of mass (located at the focus F_1) is described by:

$$r = \frac{a(1 - e^2)}{1 + e \cos \nu(t)}, \quad (2.1)$$

where a is the length of the semi-major axis for the body, e is the eccentricity, ν is the *true anomaly* the

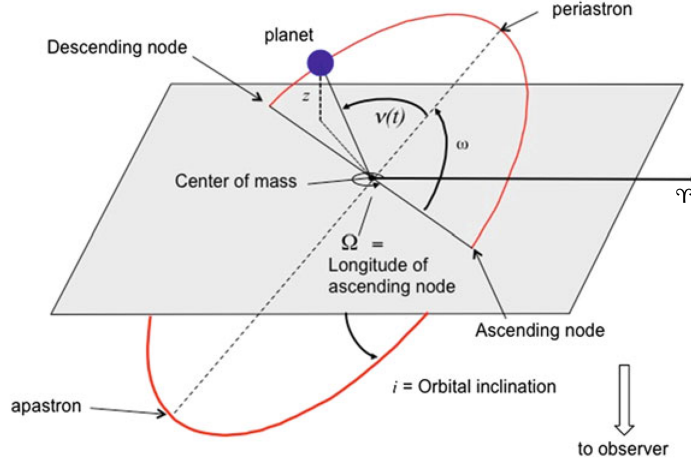


Figure 2.1: The basic elements of the Keplerian orbit. Adapted from (Bozza et al., 2016).

angle between the current position of the orbiting body and periastron.

The true anomaly is not only a function time, t , but also the orbital period P , the *time of periastron passage*, T_0 , and eccentricity. It is geometrically related to the eccentric anomaly:

$$\cos \nu(t) = \frac{\cos E(t)}{1 - e \cos E(t)} \quad (2.2)$$

which can be numerically determined from the mean anomaly $M(t)$:

$$M(t) = \frac{2\pi}{P}(t - T_0) = E(t) - e \sin E(t) \quad (2.3)$$

The mean anomaly is the angle for the average orbital motion of the body at a time after periastron passage $t - T_0$.

From Kepler's second law¹ $\frac{1}{2}r^2 d\nu/dt = \text{constant}$, while in one full period P , the total area of the ellipse $\pi a^2(1 - e^2)^{1/2}$ will be covered, leading to:

$$r^2 \frac{d\nu}{dt} = \frac{2\pi a^2(1 - e^2)^{1/2}}{P} \quad (2.4)$$

The radial velocity is the change in r along the line of sight z . The component of r along the line of sight (from Figure 2.1) is:

$$r_z = r_1 \sin(\nu_1(t) + \omega) \sin i + \gamma \quad (2.5)$$

where γ is the mean velocity of the barycentre, and the subscripts '1' and '2' refer to the star and planet (or companion star), respectively. Differentiating Equation 2.5 and substituting in Equation 2.4 leaves

¹ Orbit sweeps out equal areas in equal times

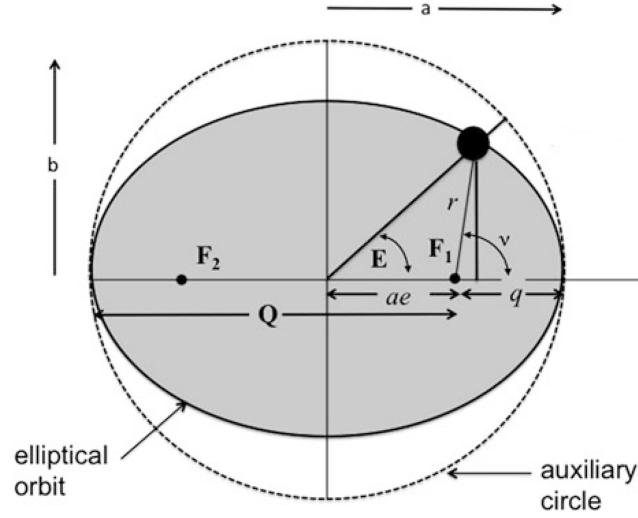


Figure 2.2: Elements of an elliptical orbit about the common centre of mass F_1 . ν is the angle to the position of the orbiting body from the periape (closest point to barycentre). The auxiliary circle has a radius equal to the semi-major axis of the ellipse. Adapted from (Bozza et al., 2016).

the common RV equation:

$$RV = \dot{r}_z = \frac{2\pi a_1 \sin i}{P(1-e^2)^{1/2}} [\cos(\nu(t) + \omega) + e \cos \omega] + \gamma \quad (2.6)$$

$$= K_1 [\cos(\nu(t) + \omega) + e \cos \omega] + \gamma, \quad (2.7)$$

where several parameters and constants have been condensed into K , referred to as the *semi amplitude*. In this case K_1 is the semi amplitude for the star.

2.1.1 Mass function

Once the orbital parameters have been determined then it is possible to determine the mass function of the system. From the centre of mass the distance between the two bodies is $a = a_1 + a_2$ where a_1 and a_2 are the respective distances to the barycentre, while the value $M_1 a_1 = M_2 a_2$ can allow these re-arrangements:

$$a = a_1 \left(1 + \frac{a_2}{a_1}\right) = a_1 \left(1 + \frac{M_1}{M_2}\right) = \frac{a_1}{M_2} (M_1 + M_2) \quad (2.8)$$

Kepler's third law ($G(M_1 + M_2)/4\pi^2 = a^3/P^2$) can be written as:

$$\frac{G(M_1 + M_2)}{4\pi^2} = \frac{a_1^3}{P^2} \left(\frac{M_1 + M_2}{M_2}\right)^3 \quad (2.9)$$

Table 2.1: The RV semi-amplitude induced by the planets with different masses and periods around a $1 M_{\odot}$ -mass star.

M_2	$K_1(P = 3 \text{ d})$	$K_1(P = 1 \text{ yr})$	$K_1(P = 5 \text{ yr})$	
M_{Jup}	140.8	28.4	16.6	m s^{-1}
M_{Nep}	7.60	1.53	0.90	m s^{-1}
M_{\odot}	44.3	8.9	5.2	cm s^{-1}

replacing a_1 with K_1 from Equation 2.6 results in the *mass function*, $f(M)$:

$$f(M) = \frac{(M_2 \sin i)^3}{(M_1 + M_2)^2} = \frac{K_1^3 P (1 - e^2)^{3/2}}{2\pi G} \quad (2.10)$$

This function can be determined directly from the measurable parameters P , e and K_1 . It also depends on the stellar mass M_1 , which needs to be measured by some other means to determine the planet mass. Also from this function that the true mass of the planet M_2 is not obtained but only the projected mass $M_2 \sin i$.

For a planetary companion the approximation $M_2 \ll M_1$ can be made and for circular orbit the radial velocity semi-amplitude can be re-written as:

$$K_1 = \frac{28.4}{\sqrt{1 - e^2}} \frac{M_2 \sin i}{M_{\text{Jup}}} \left(\frac{M_1}{M_{\odot}} \right)^{-2/3} \left(\frac{P}{1 \text{ yr}} \right)^{-1/3} [\text{m s}^{-1}] \quad (2.11)$$

This can be used to calculate the RV amplitude created by different mass planets in various circular orbits as given in Table 2.1. The recently commissioned ESPRESSO optical spectrograph is designed with the goal of achieving 10 cm s^{-1} , which is the level of precision required to detect an Earth mass planet in an 1 year orbit round a Sun-like star.

If there is more than one companion/planet then there will be a gravitational influence between each other and their orbits become non-Keplerian, i.e. a N-body problem (e.g. Chenciner, 2007). Assuming that the gravitational influence between companions is negligible the RV signal observed in the host star can be treated as just a sum of tugs from each companion. For the two instances in this work where the target star has two companions, the companions will be treated separately, as if they were alone.

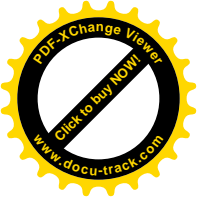
2.1.2 Binary mass ratio

In the above equation RV of the companion has not yet been addressed. Equation 2.6 above is the RV of the star in an elliptical orbit around the centre of mass between it and its companion. Similarly the elliptical orbit of the planet around the centre of mass is given by:

$$RV_2 = K_2 [\cos(\nu(t) + \omega_2) + e \cos(\omega_2)] + \gamma, \quad (2.12)$$

where $\omega_2 = \omega + 180^\circ$ due to the phase difference between the two components, resulting in the relative velocity (ignoring γ) of the companion being opposite the star and:

$$K_2 = \left(\frac{2\pi G}{P(1 - e^2)^{3/2}} \right)^{1/3} \frac{M_1 \sin i}{(M_1 + M_2)^{2/3}} = \frac{2\pi a_2 \sin i}{P(1 - e^2)^{1/2}} \quad (2.13)$$



The orbits of the host and companion are directly related through the mass ratio of the star and companion:

$$q = \frac{M_2}{M_1} = \frac{K_1}{K_2} = \frac{RV_1}{RV_2} = \frac{r_2}{r_1}. \quad (2.14)$$

Typically in exoplanet detections the companion (planet) is **two** faint to measure the planetary velocity. However in double lined spectroscopic binary the spectrum of both stars can be identified in the blended spectra and the RV of both star and companion can be measured and monitored over the orbit. With both velocities the mass ratio of the binary can be found. The individual masses however **is** still not determinable due to the inclination $\sin i$ of the orbit.

In Chapter 6 the detection of the faint spectra **is** of known companions is attempted, in order to determine the velocity change of the companion and hence the mass ratio. To help with the analysis and simulations the known orbital parameters (see Tables 6.1 and 6.2) are used along with the companion mass (M_2 or $M_2 \sin i$) to predict or estimate the RV of the companion using Equations 2.12 and 2.14. Note, that for the targets in which only the minimum mass ($M_2 \sin i$) is known and used in the mass ratio, this will result in the maximum RV semi amplitude for the companions **orbit**. The estimated K_2 for each companion is provided in Table 6.4 while the RV for both components at the time of each observation is provided in Table 6.3.

2.2 Measuring the RV

The motion of the star towards and away from the Earth shifts the lines of its spectra through the Doppler Effect. In the non-relativistic limit this can be written as:

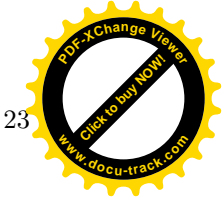
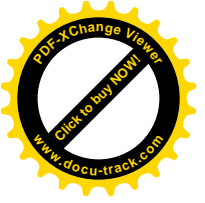
$$\frac{\Delta\lambda}{\lambda} = \frac{v}{c}, \quad (2.15)$$

where $\Delta\lambda$ is the wavelength shift of wavelength λ with a velocity relative to the observer of v . The *speed of light* is the constant c . To measure the RV the relative positions of the stellar lines need to be measured over time. Typically this is done via the cross-correlation (CCF) of the observed spectrum with a template mask (e.g. a binary mask (Baranne et al., 1996) or weighted mask (Pepe et al., 2002)) suitable for the spectral type of the observed star. The CCF stacks together the spectral lines **crating** **and** “average” line, reducing the random noise on the individual N spectral lines by a factor of \sqrt{N} . The CCF collapses the RV from all the lines into one number with higher precision than individual lines.

2.3 RV precision

To achieve a high-level RV precision, two sources of noise must be controlled: statistical error **form** the RV measurement and systematic errors induced by the spectrograph. This requires a stabilized spectrograph, precisely calibrated in wavelength, and the combination of thousands of lines (e.g. Pepe et al., 2014b). The fundamental source of noise is photon noise, which follows a Poisson distribution. That is, an observable with an average value of N has a standard deviation \sqrt{N} .

A very general formula for the RV precision achievable of a given spectrum, in terms of general



spectral parameters is given by Hatzes et al. (1992) as:

$$\sigma \propto \frac{1}{\sqrt{F}\sqrt{\delta\lambda}R^{1.5}}. \quad (2.16)$$

\sqrt{F} represents the signal-to-noise ratio (SNR) of the spectrum in the **poison**-dominated noise regime, while $\Delta\lambda$ is the bandwidth of the observed spectrum. This assumes that the spectrum contains a homogeneous distribution of uniform lines, per unit wavelength. The precision depends more steeply on the spectral resolution with $R^{-1.5}$ occurring due to the bandwidth and the number of lines visible on a fixed detector size decreases with increased resolution. In high resolution RVs this tends to R^{-1} indicating the higher precision at the expense of wavelength coverage is desired Hatzes et al. (1992). As a star rotates its lines become broadened by an area preserving rotation kernel (see Section 8.1.3). In a similar way to the resolution the RV precision is dependant on rotational velocity of the star ($v\sin i$) to the power 1.5.

Assuming a spectral line is comprised of Gaussian-shaped absorption lines **if** the precision of a line can be shown to be:

$$\sigma \sim \frac{\sqrt{\text{FWHM}}}{C \cdot \text{SNR}} \quad (2.17)$$

where FWHM is the full width at half maximum of the line, C is the line contrast (depth relative to continuum) and SNR the signal-to-noise of the continuum. An alternate derivation comes from Bouchy et al. (2001) in which the optimal weight for each pixel is calculated for a spectrum A_0 via:

$$W(i) = \frac{\lambda^2(i)(\partial A_0(i)/\partial \lambda)^2}{A_0(i) + \sigma_D} \quad (2.18)$$

with the RV precision calculated over all pixels as

$$\delta v_{RMS} = \frac{c}{\sqrt{\sum_i W(i)}}. \quad (2.19)$$

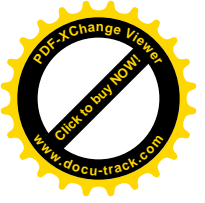
where λ the wavelength and σ_D the detector noise.

In all these formulations there are some key properties to achieve high RV precision: a high stellar flux F to achieve a high SNR, observed at high resolution to have sharp spectral line. The deeper (high C) and narrower (small FWHM) a spectral line², the better defined the position of the line will be, allowing for a higher precision measurement of the RV. The flux F or SNR of an observation increases with the number of photons collected which depends on the stellar brightness as well as distance³, coupled with the telescope size and with the exposure time. This limits the highest precision RV measurements to relatively nearby stars. Cross-dispersed echelle spectrographs mounted on the largest telescopes are capable of delivering the high-resolution, high SNR and high bandwidth requirements necessary to achieve high precision RV measurements.

These formula have recently been used to assess the theoretical RV precision of synthetic spectra for the development of instrument designs of new nIR spectrographs (e.g. Figueira et al., 2016) as well as compare precision of real and synthetic spectra (e.g. Artigau et al., 2018). The RV precision will be

² With steeper gradients $\partial A_0(i)/\partial \lambda$.

³ Basically the stars apparent magnitude



analysed further in Chapter 8 with a detailed derivation of the Bouchy et al. (2001) method given and implemented to analyse the precision of nIR spectra.